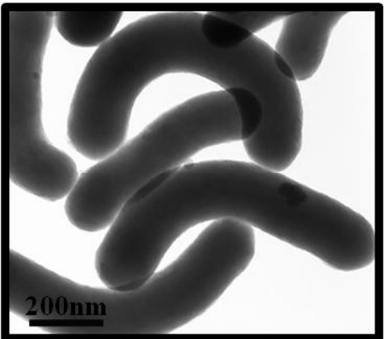
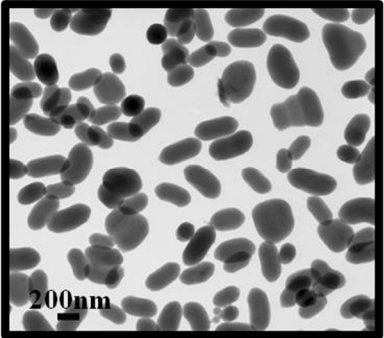
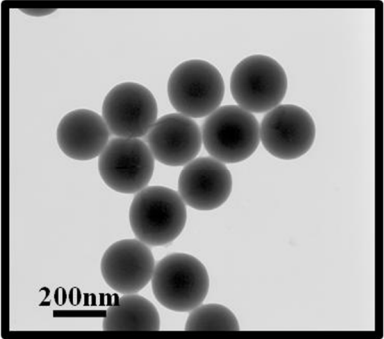


Supporting Information.

SUPPLEMENTAL FIGURES:

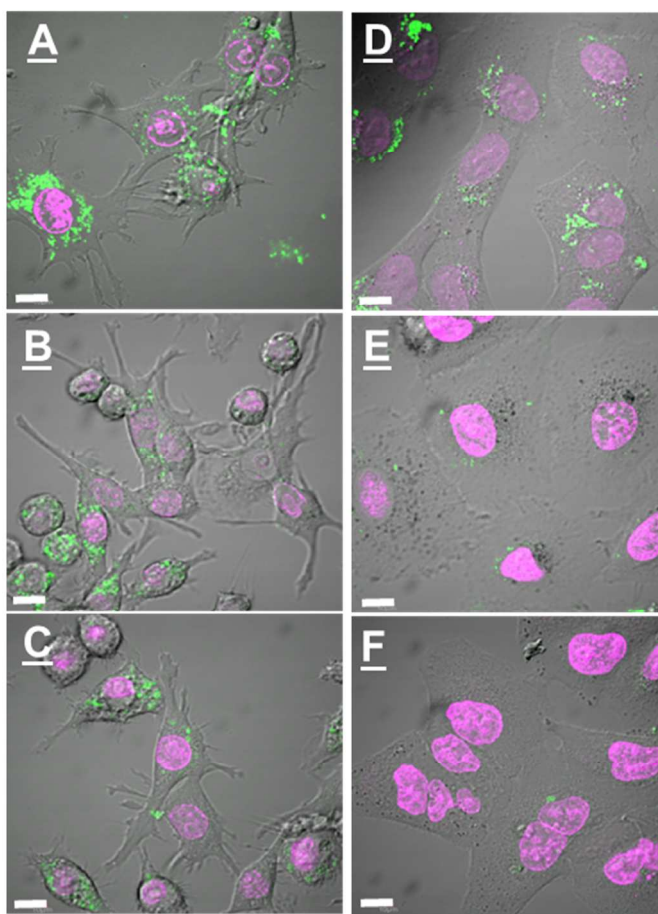
Nanoparticle	Size (TEM)	Dynamic Light Scattering (DLS)	Dynamic Light Scattering in Media Containing Serum	Fluorescent Units Per Particle	Zeta Potential	Zeta Potential in Media Containing Serum	TEM Images
<i>Worms</i>	232 ± 22 nm x 1348 ± 314 nm	598.2 ± 119.8 nm*	583 ± 292 nm**	~11 units per particle***	87 mV	-8 mV**	
<i>Cylinders</i>	214 ± 29 nm x 428 ± 66 nm	369 ± 85 nm*	511 ± 128 nm**	~9 units per particle***	79 mV	-8 mV**	
<i>Spheres</i>	178 ± 27 nm	240 ± 20 nm	355 ± 162 nm**	~8 units per particle***	58 mV	-8 mV**	

*Please note that these particles are not spherical, so the information may not reflect the actual particle configuration, as the DLS theory assumes spherical conformation.

**Serum proteins are also present in significant quantities so results may not reflect the measurements of just the particles or the attachment of the proteins to the surface of the particles. Due to the presence of multiple peaks in the spectra, only the most relevant peak is reported that was

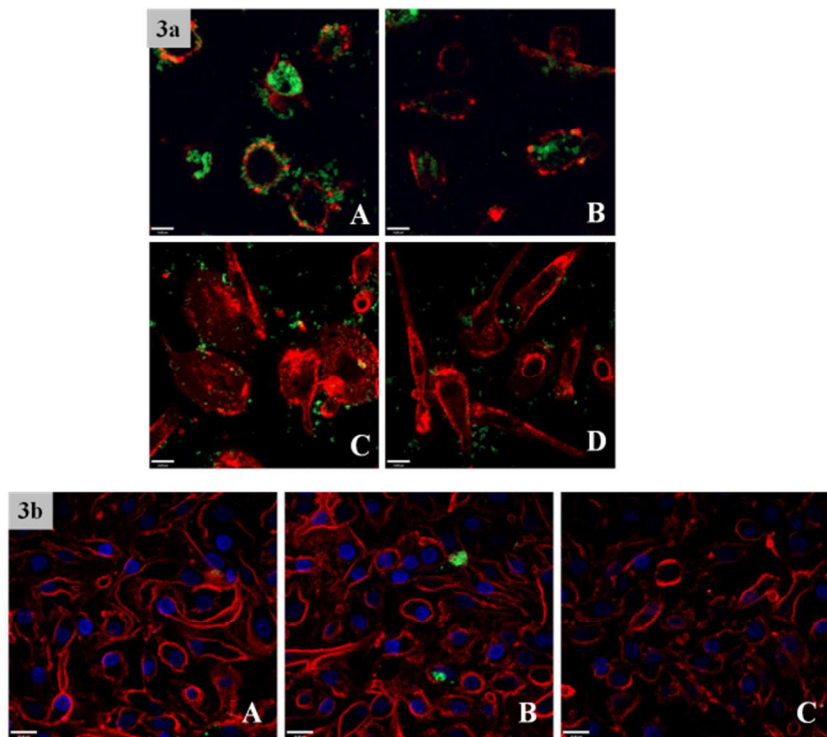
not present in just media containing serum.***Fluorescent units were determined utilizing a standard fluorescence curve of known FITC concentration. The fluorescence per particle was determined by a back calculation utilizing the surface area of each particle and a density of 2.6 g/mL for silica nanoconstructs.

Supplemental Figure 1 and Supplemental Table 1¹: Physicochemical Characteristics of Silica Nanoparticles and Transmission Electron Microscope (TEM) images of aqueous suspensions of silica nanoconstructs. A) Worms; B) Cylinders; C) Spheres.



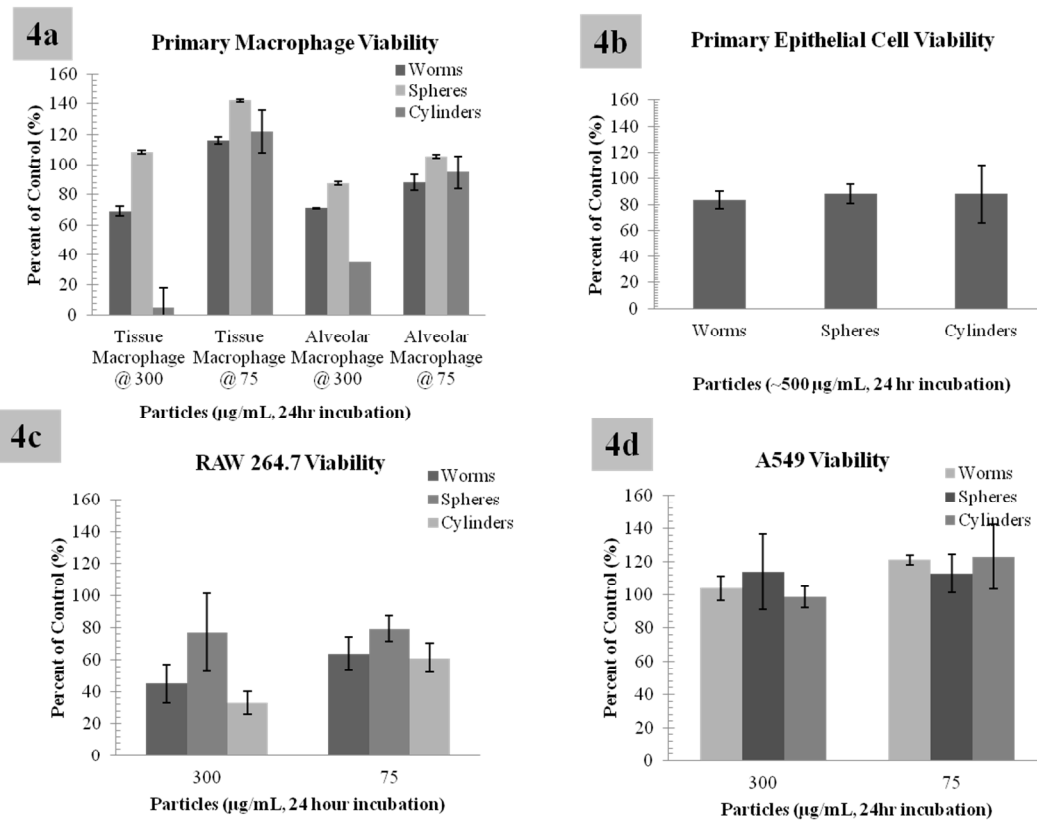
Supplemental Figure 2 (modification¹): Confocal images of 50 $\mu\text{g/mL}$ silica nanoconstruct uptake after 24 hours of incubation in RAW264.7 (left) and A549 cells (right). Cell nucleus in

pink and particles in green A and D) Worms; B and E) Cylinders; C and F) Spheres. All nanoparticles were observed to be taken up into cells. Scale bar 10 μ m.



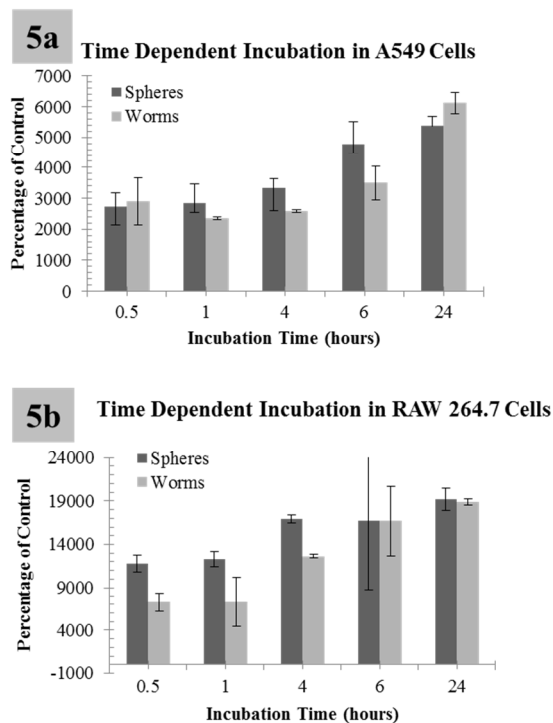
Supplemental Figure 3: Confocal image analysis of preliminary uptake of nanoparticles within primary cells. **3a:** Primary macrophage confocal image (membrane stained red) uptake of silica nanoparticles (green). A and B) Alveolar macrophages treated with 75 μ g/mL of spherical and worm like nanoparticles, respectively. C and D) Tissue macrophages treated with 75 μ g/mL of spherical and worm like nanoparticles, respectively. Alveolar macrophages (A and B), as this figure demonstrates when correlated to our FACS analysis in Figure 1, there is a greater degree of nanoparticle uptake when compared to tissue macrophage uptake where much of fluorescence was associated with the cell membrane (C and D). It is also important to note that macrophages treated with spherical nanoparticles (A and D) when compared to worm like nanoparticles (B and D) appear to have a greater degree of nanoparticle uptake (at this time point, 1.5 hours). This

suggests a phenotypic and geometric implication. **3b**: Confocal image of uptake of silica nanoparticle constructs in alveolar epithelial cells; limited uptake of silica nanoconstructs was observed in primary epithelial cells similar to what is observed in FACS results presented in Figure 1b. Particles (green) at a concentration of 50 μ g/mL were incubated with primary alveolar epithelial cells for two hours, following incubation to help with cellular visualization of the cell membrane stained with Rhodamine-WGA (red) and nucleus stained with DAPI following cellular fixation; A) Cylinder incubation, B) Spherical incubation, C) Worm incubation. Scale bar = 14.0 μ m.



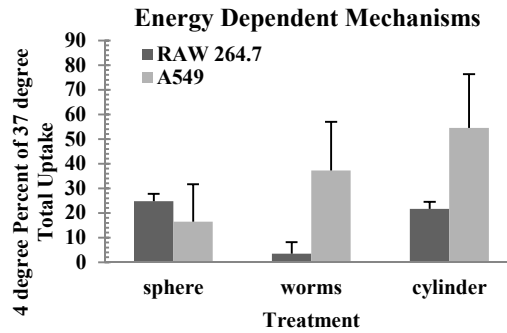
Supplemental Figure 4: Vialight assay, assessing the relative ATP level in metabolically active cells. **4a** and **4b**: Vialight assay, assessing the relative ATP level in metabolically active cells. . In **4a**, macrophages exhibit a varied response. When exposed to high concentrations of silica

nanoparticle constructs they exhibit a degree of toxicity while they appear to tolerate lower concentrations. As shown in **4b**, alveolar epithelial cells show very little decrease in cell viability when exposed to silica nanoparticle constructs **4c**: RAW 264.7 macrophages exhibit a varied response. When exposed to high concentrations of silica nanoparticle constructs they exhibit a degree of toxicity while tolerating lower concentrations. **4d**: A549 epithelial cells show very little decrease in cell viability when exposed to silica nanoparticle constructs. Please note: graphs are represented as percentage of control or the background viability of cells incubated without nanoparticles.

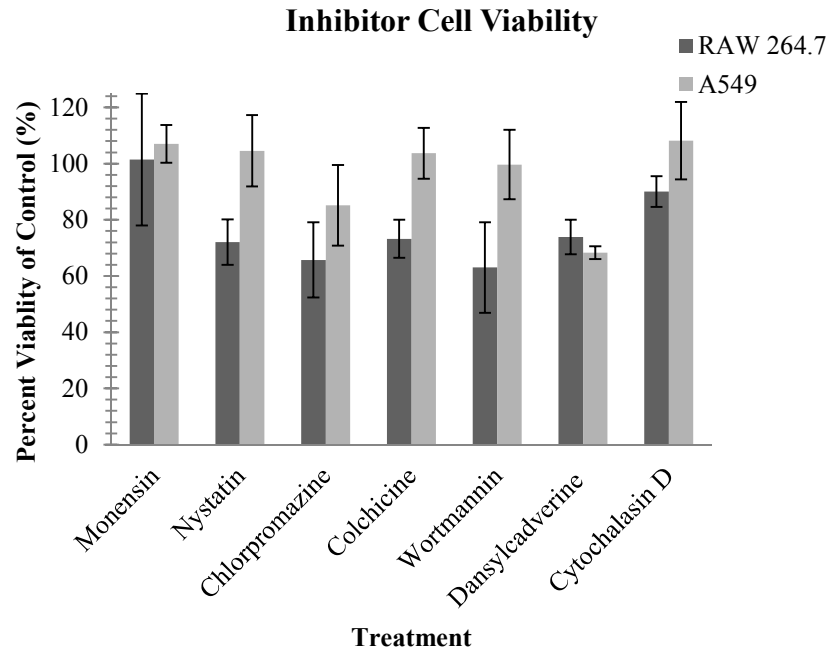


Supplemental Figure 5: Time dependent fluorescence uptake of silica nanoparticles. **5a and 5b)** All time points tested of 75 $\mu\text{g}/\text{mL}$ in RAW 264.7 cells and A549 cells respectively. A gradual increase in concentration uptake was observed in cells until a concentration threshold was achieved. Above this threshold cells no longer took up nanoparticles. Please note: graphs

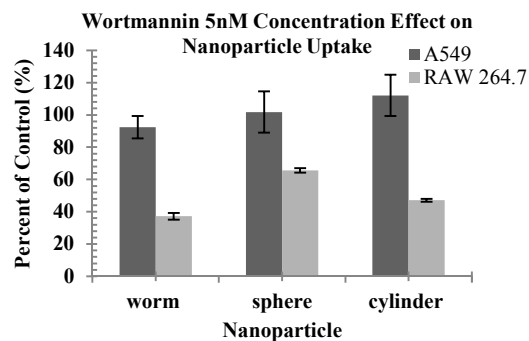
are represented as percentage of control or the background provided by FACS analysis of cells incubated without nanoparticles. Low levels of autofluorescence were indicated for immortalized lines.



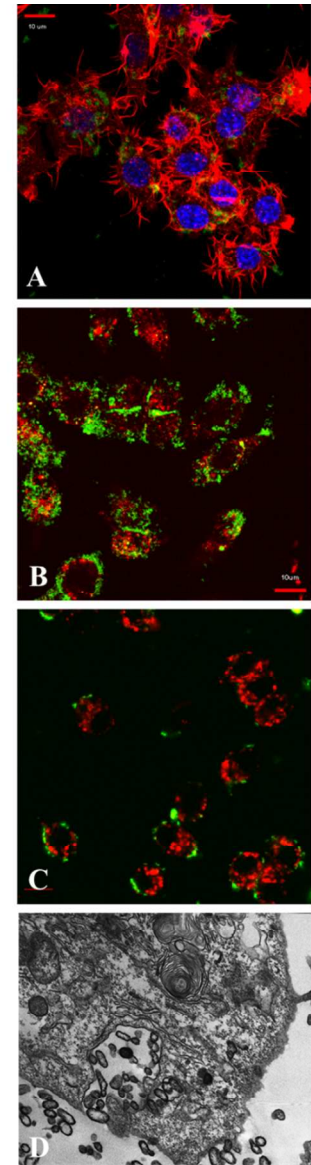
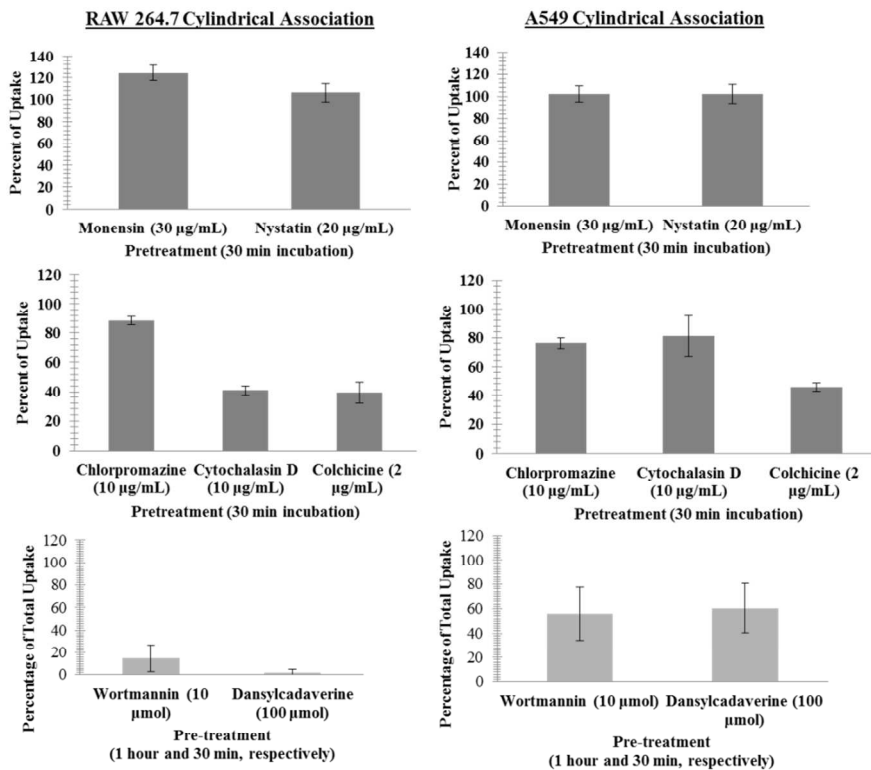
Supplemental Figure 6: Representative image of the relative uptake of nanoparticles as a function of temperature in model cell lines. The graph provides confirmation of energy dependent mechanisms of uptake. Please note: graph is represented as percentage of uptake at 37 degrees of the respective nanoparticle at 4 degrees. So at 4 degrees RAW 264.7 cells exhibit ~25% of the spherical uptake that they exhibit at 37 degrees.



Supplemental Figure 7: Vialight assay, assessing the relative ATP level in metabolically active cells after treatment with inhibitors. Caveolin dependent endocytosis was assessed utilizing Nystatin at a 30 minute pre-incubation at 20 $\mu\text{g}/\text{mL}$. Clathrin dependent endocytosis was assessed utilizing a 30 min pre-incubation with either 100 μmol of Dansylcadaverine or 10 $\mu\text{g}/\text{mL}$ of Chlorpromazine. Clathrin and caveolin independent endocytosis were assessed utilizing a 30 minute pre-treatment with 30 $\mu\text{g}/\text{mL}$ Monensin. Phagocytosis and macropinocytosis were assessed utilizing a 1 hour incubation with 10 μmol or 10 nmol concentrations of Wortmannin or a 30 minute pre-incubation with 2 $\mu\text{g}/\text{mL}$ of Colchicine. Please note: graph is represented as a percentage of control or cell viability without inhibitor incubation.

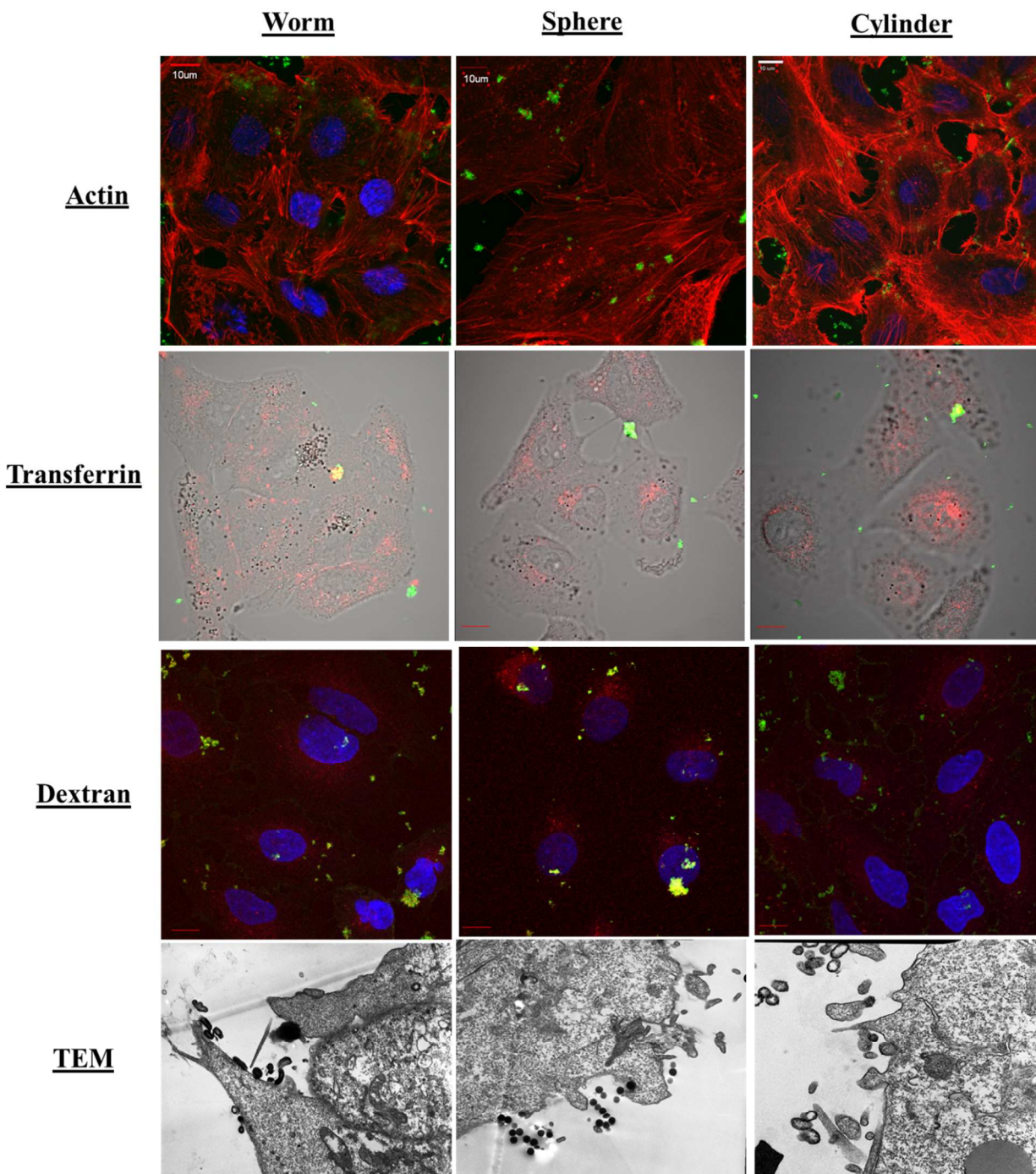


Supplemental Figure 8: An additional lower concentration of wortmannin was tested to discern between phagocytic and macropinocytic uptake. However, very little differences between the two concentrations were observed. Please also note: graphs are represented as percentage of uptake or the background provided by FACS analysis of cells incubated with the respective nanoparticles without the wortmannin inhibitor.

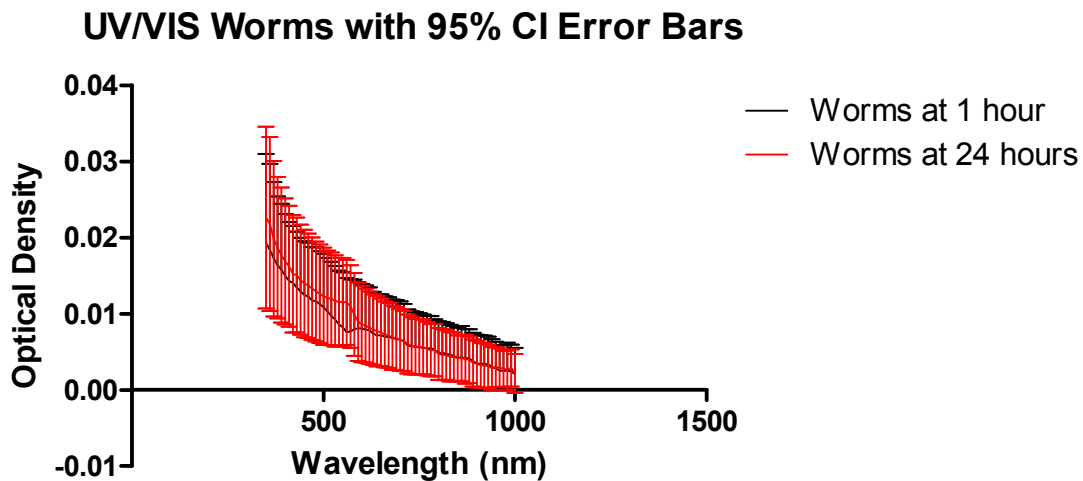
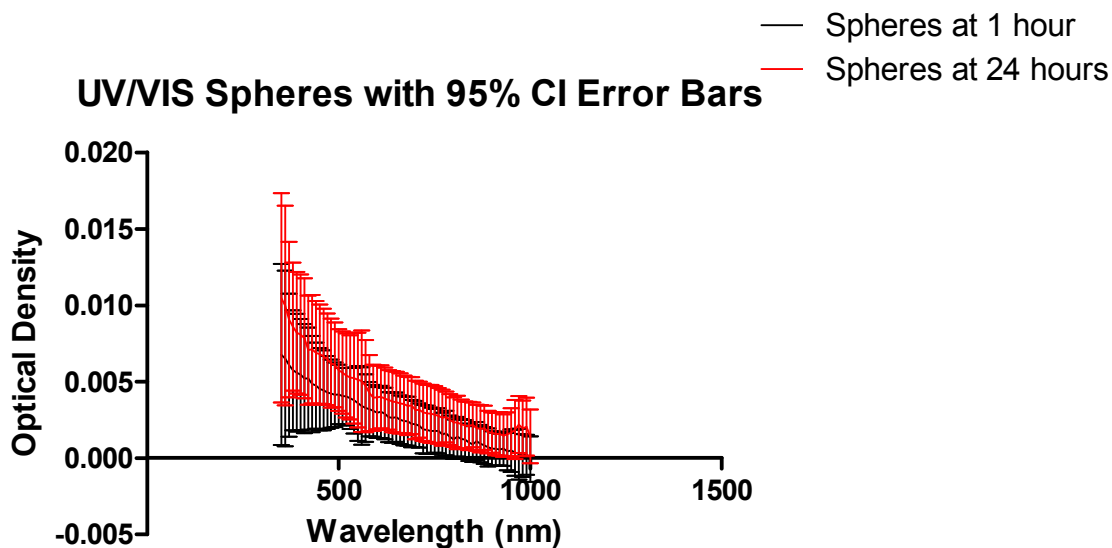


Supplemental Figure 9: Cylindrical data was similar to worm like particles. Left are the impact of inhibitor treatments on cylindrical uptake. A) Actin staining with cylindrical treatment in RAW 264.7 cells, B) Dextran staining with cylindrical treatment in RAW 264.7 cells, C) Transferrin staining with cylindrical treatment RAW 264.7 cells, and D) TEM images of cylindrical treatment RAW 264.7 cells. Please see main text for complete experimental details and explanations. Please also note: graphs are represented as percentage of uptake or the

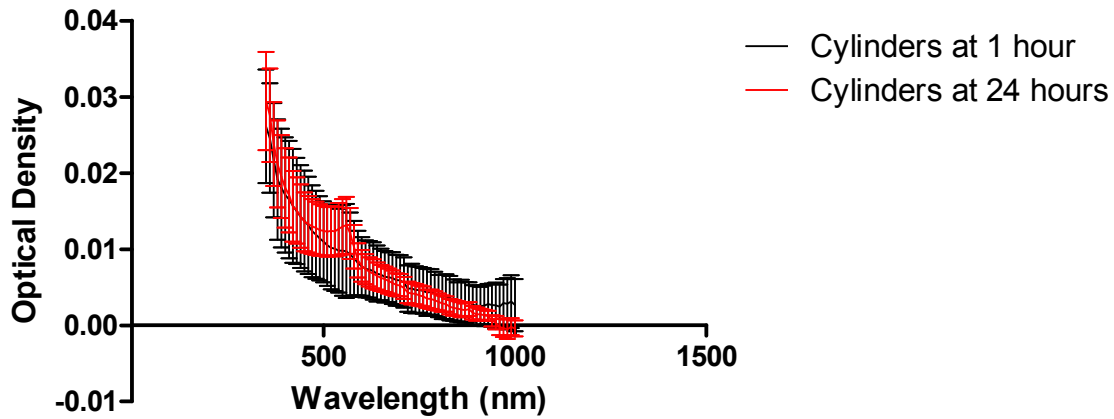
background provided by FACS analysis of cells incubated with cylinders without the respective inhibitor.



Supplemental Figure 10: A549 data to supplement the RAW 264.7 data outlined in the paper, due to the similarities of the images, these were excluded from the publication. Please see main text for complete experimental details and explanations.



UV/VIS Cylinders with 95% CI Error Bars



Supplemental Figure 11: Spectrophotometric stability tests in media, at incubation times of 1 and 24 hours, spectrophotometric measurements of media alone at these time points has been subtracted. Error bars represent a 95% confidence interval of 9 samples incubated at each time point. Overlap of this interval indicates stability of particles (limited to no aggregation) in media over incubation time periods.

SUPPLEMENTAL TABLE:

2a:

Tissue Macrophage Worm Treatment	Tissue Macrophage Sphere Treatment	Alveolar Macrophage Worm Treatment	Alveolar Macrophage Sphere Treatment	GO Analysis	MESH Analysis	KEGG Analysis
	AKT1			Regulation of Cell Growth, Cell Growth, Regulation of Cell Size and Shape, Cellular Morphogenesis, Signal transduction, Cell Communication, Cell Surface Receptor Linked Signal Transduction	Phosphoproteins	Insulin Signaling Pathway, Focal Adhesion, Apoptosis, Toll-like Receptor Signaling Pathway
AKT3	AKT3			Protein Amino Acid Phosphorylation, Phosphorylation, Phosphorus Metabolism, Signal Transduction, Cell Communication		Apoptosis, Toll-like Receptor Signaling Pathway, Insulin Signaling Pathway, Focal Adhesion
	BAD					Apoptosis
	CASP9					Apoptosis

CSNK2A1	CSNK2A1			Protein Amino Acid Phosphorylation, Phosphorylation, Phosphorus Metabolism, Cellular Morphogenesis, Cell Growth and Regulation	Phosphoproteins	
CTNNB1	CTNNB1			Signal Transduction, Cell Communication, Signal Transduction, Cell Surface Receptor Linked Signal Transduction		Focal Adhesion
	EIF4B					
EIF4EBP1	EIF4EBP1			Signal Transduction	Phosphoproteins	Toll like Receptor Signaling Pathway, Insulin Signaling Pathway
FOXO3	FOXO3					
	JUN					Focal Adhesion, Toll-like Receptor Signaling Pathway
MTOR	MTOR			Protein Amino Acid Phosphorylation, Phosphorylation, Phosphorus Metabolism, Cellular Proliferation	Ribosomal Protein S6 Kinases, Phosphoproteins	
ITGB1	ITGB1			Signal Transduction, Cell Communication, Cell Surface Receptor Linked Signal Transduction		Focal Adhesion
PABPC1	PABPC1					
	PAK1			Signal Transduction, Cell Communication		Focal Adhesion
	PTEN			Regulation of Body Size, Cell Growth	Phosphoproteins	Focal Adhesion
SHC1	SHC1			Signal Transduction, Protein Kinase Cascade, Regulation for Cell Size and Growth, Cellular Morphogenesis, Cell Proliferation		Insulin Signaling Pathway, Focal Adhesion
			SOS1			

2b:

Tissue Macrophage Worm Treatment	Tissue Macrophage Sphere Treatment	Alveolar Macrophage Worm Treatment	Alveolar Macrophage Sphere Treatment	GO Analysis	MESH Analysis	KEGG Analysis
B2M	B2M					
		BAD				Insulin Signaling Pathway, Apoptosis
		CDKN1B				
CHUK		CHUK		Protein Amino Acid Phosphorylation, Phosphorylation, Phosphorus Metabolism, Signal Transduction, Cell Communication, Protein Kinase Cascade, NF-kappa B Cascade		Insulin Signaling Pathway, Apoptosis, Toll-like Receptor Signaling Pathway
			ELK1			
FASLG		FASLG		Signal Transduction, Protein Kinase Cascade, NF-kappa B Cascade		Apoptosis

IGF1				Signal Transduction		Focal Adhesion
		IRS1				Insulin Signaling Pathway,
MAPK3				Protein Amino Acid Phosphorylation, Phosphorylation, Phosphorus Metabolism	Ribosomal Protein S6 Kinases	Insulin Signaling Pathway, Focal Adhesion
MYD88	MYD88			Signal Transduction, Cell Communication, Protein Kinase Cascade, NF-kappa B cascade		Toll-like Receptor Signaling Pathway, Apoptosis
NFKB1	NFKB1		NFKB1	Signal Transduction, Cell Communication, Protein Kinase Cascade, Response to Pathogenic Bacteria		Toll-like Receptor Signaling Pathway, Apoptosis
NFKBIA				Signal Transduction, Cell Communication, NF-kappa B Cascade, Response to Pathogenic Bacteria		Toll-like Receptor Signaling Pathway, Apoptosis
			PABPC1			
		PDK2				
PIK3CA				Protein Amino Acid Phosphorylation, Phosphorylation, Phosphorus Metabolism, Signal Transduction, Cell Communication		Insulin Signaling Pathway, Toll-like Receptor Signaling Pathway, Focal Adhesion
PIK3CG	PIK3CG			Protein Amino Acid Phosphorylation, Phosphorylation, Phosphorus Metabolism, Signal Transduction, Cell Communication	Ribosomal Protein S6 Kinases, Phosphoproteins	Insulin Signaling Pathway, Apoptosis, Focal Adhesions, Toll-like Receptor Signaling Pathway
PIK3R1		PIK3R1		Signal Transduction, Cell Communication		Insulin Signaling Pathway, Apoptosis, Focal Adhesions, Toll-like Receptor Signaling Pathway
		PIK3R2				Insulin Signaling Pathway, Apoptosis
PRKCB				Protein Amino Acid Phosphorylation, Phosphorylation, Phosphorus Metabolism, Signal Transduction, Cell Communication		Focal Adhesion
RASA1				Signal Transduction, Cell Communication		
	RBL2				Phosphoproteins	
	RHEB			Cell Surface Receptor Linked Signal Transduction, Cell Growth, Cell Communication		
RPS6KB1	RPS6KB1			Protein Amino Acid Phosphorylation, Phosphorylation, Phosphorus Metabolism, Signal Transduction, Cell Communication		
		TCL1A				
TLR4	TLR4			Signal Transduction, Cell Communication, Protein Kinase Cascade, NF-kappa B cascade, Response to Pathogenic Bacteria		



Supplemental Table 2: 2a: Up-regulated genes in PI3-kinase pathway are exposed to data mining tools through the program GATHER². **2b:** Down-regulated genes. Some overlaps are observed in the regulated genes.

SUPPLEMENTAL REFERENCES:

1. Herd, H. L.; Malugin, A.; Ghandehari, H., Silica nanoconstruct cellular toleration threshold in vitro. *J Control Release* **2011**, 153, 40-48.
2. Chang, J. T.; Nevins, J. R., GATHER: a systems approach to interpreting genomic signatures. *Bioinformatics* **2006**, 22, 2926-2933.